

**GIS and Machine Learning Approaches in Flood Hazard Mapping: A Case Study of Lower
Niger River Basin**

***¹Adeyemi, Adedoyin Benson and ¹Komolafe, Akinola Adesuji**

¹Department of Remote Sensing and Geoscience Information System (GIS), Federal University
of Technology, Akure, Nigeria

*Corresponding Author's Email: abadeyemi97@gmail.com, Phone No.: +2348141154368

ABSTRACT

Flooding is a recurrent and destructive natural disaster intensified by elements such as extreme rainfall, urbanization, climate change, topography, and human activities. This study primarily aims to integrate Geographic Information System (GIS) and Machine Learning (ML) techniques in flood hazard mapping in the lower Niger River basin in Nigeria. Twenty flood influencing factors including elevation, slope, aspect, flow direction, flow accumulation, drainage density, distance from river, plan curvature, profile curvature, roughness, topographic wetness index (TWI), stream power index (SPI), sediment transport index (STI), normalized difference vegetation index (NDVI), normalized difference moisture index (NDMI), land use/land cover (LULC), soil, geology, temperature, and rainfall, were considered and analyzed within the GIS framework. The Extreme Gradient Boosting (XGBoost) model was applied to generate the flood hazard zones within the study area. Based on historical flood events within the study area, 1164 flooded and non-flooded points were identified and utilized to train and test the model. The ML model achieved high accuracy of 0.905 (90.5%), and an ROC-AUC score of 0.88. The generated flood susceptibility map indicated that 4.67%, 4.98%, 10.31%, 11.13%, and 68.91% of the basin are respectively at very high, high, moderate, low, and very low risk of flooding. The successful integration of GIS with machine learning validates the potential to improve flood hazard prediction and mitigation efforts in the Niger River basin and other similar flooding environments in Nigeria.

Keywords: Flood Hazard Mapping, Geographic Information System, Machine Learning, XGBoost, Niger River Basin

1.0 INTRODUCTION

Globally, flood is acknowledged to be one of the most frequent and devastating natural hazards that endangers human lives, property, and infrastructure (Ibitoye *et. al.*, 2020). Across the globe, floods inflict unimaginable agony on people and economic hardship (Ghosh *et. al.*, 2023). The United Nations Platform for Space-based Information for Disaster Management and Emergency Response (UN-SPIDER) in 2019, referred flooding to be the presence of water where it is not wanted. It often occurs when a river or water body exceeds its capacity. In 2022, the World Bank accounted for over 1.81 billion people across the globe to be directly exposed to flooding at a depth of over 0.15m. Significant economic and human losses result from the annual increase in the frequency of floods, which is made worse by intense precipitation, climate change, and fast urbanization. Although there are benefits to flooding, such as improved soil fertility,

41 replenished water supplies, and the development or restoration of habitats for a variety of
42 animals and plants, (Aldardasawi and Eren, 2021; Maharjan *et. al.*, 2024), the drawbacks of
43 flooding are arguably greater than the benefits. The physical geography of low-lying coastal areas
44 and river floodplains, which have consistently drawn human settlement over time, forms the
45 basis for the phenomenon of flooding causing economic damage. The movement of people from
46 rural to urban areas, or within cities, often leads them to settle in locations highly prone to
47 flooding, thereby increasing their susceptibility in the absence of adequate flood defense
48 mechanisms (Jha *et. al.*, 2022).

49 While the occurrence of flood spans across latitudes and longitudes, Nigeria is a prime example
50 of a country facing the tremendous difficulties brought on by frequent floods. Flooding has been
51 shown to have caused millions of deaths, destroyed businesses, poisoned water sources,
52 increased the risk of sickness in several parts of Nigeria (Etuonovbe, 2011), and caused
53 destruction of farmlands thereby having negative impacts on food security. The disruptive
54 impacts of flooding are especially dangerous for Nigeria's agriculture industry. Large swaths of
55 agricultural area are often submerged, resulting in crop failures and lower yields. Recent
56 experiences in the nation indicate that the disastrous floods that occurred in 2012 and 2022 were
57 the worst (Adaji *et. al.*, 2019). Over 14 states in the nation were reported to have been impacted
58 by the 2012 flood (Tokunbo and Ezigbo, 2012). According to EM-DAT, the flood in 2012 was
59 estimated to have impacted 7,000,867 lives, resulted in 363 fatalities, and caused economic
60 damages of roughly \$500,000 (Guha-Sapir *et. al.*, 2013; Komolafe *et. al.*, 2015). Nigeria has seen
61 more frequent and severe floods recently, especially in the Niger River Basin. There are
62 noticeable seasonal changes in the water level of the Niger River. Flood dangers are increased by
63 this large floodplain and the tropical environment that is marked by heavy rainfall such as the
64 Niger River basin. This necessitates the need for comprehensive nonstructural measures to assess
65 the potential flood risk associated with the basin.

66 The utilization of GIS technology, by integrating geospatial datasets helps understand the
67 complex interplay of flood-influencing factors and the invaluable insights it offers in flood
68 hazard assessment and management (Komolafe *et. al.*, 2020). Machine learning which is referred
69 to be a subsection of Artificial Intelligence serves as an influential tool in extracting patterns and
70 knowledge from large datasets by learning from the data (Ighile *et. al.*, 2022). An effective way
71 to enhance flood risk assessments is by utilizing GIS and machine learning to integrate several
72 geographic datasets, such as those related to topography, hydrology, climate, environmental, and
73 anthropogenic features (Edamo *et. al.*, 2022). Creating more precise and educational flood hazard
74 maps is feasible when GIS spatial analytic skills are combined with machine learning prediction
75 capacity. This study aims to integrate Geographic Information System (GIS) and Machine
76 Learning (ML) techniques in flood hazard mapping in the lower Niger River basin in Nigeria.

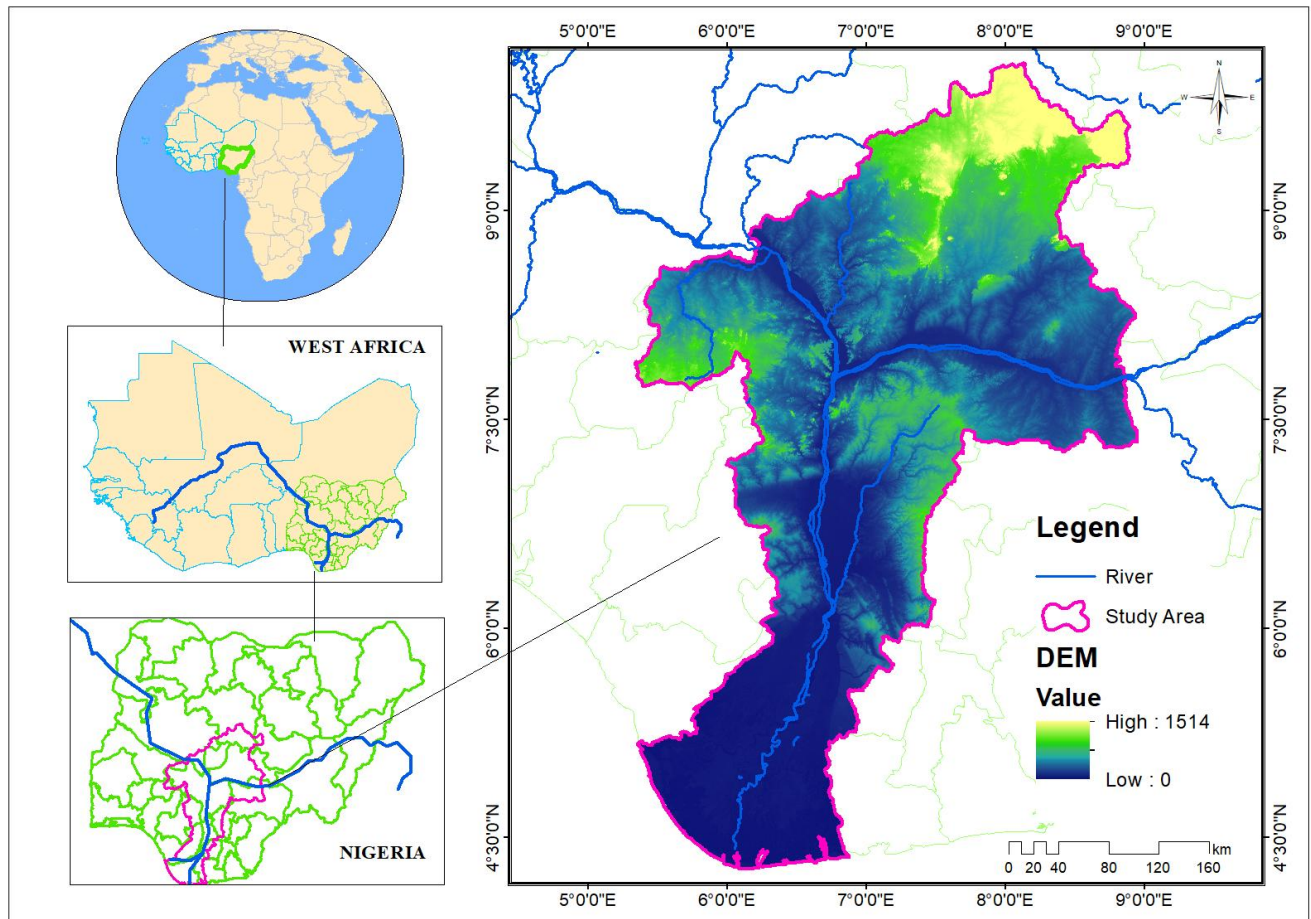
77

78 **2.0 STUDY AREA**

79 The area considered for this study is the combination of sub-basins of the Niger River in Nigeria
80 (Figure 1). The area covers parts of 15 States of the Country, descending from the North-Central

81 to the South-South. The study area is located between Latitudes $9^{\circ}30'0''$ N and $4^{\circ}28'0''$ N, and
82 Longitudes $5^{\circ}0'0''$ E and $9^{\circ}0'0''$ E. The main Niger River being the largest river basin of western
83 Africa runs in a crescent shape from the Guinea Highlands in Guinea, through Mali, Niger, and
84 then Nigeria where it joins with the Benue River, its main tributary. The vast hydrological system
85 of the Niger River, characterized by its susceptibility to frequent and severe flooding, offers an
86 unparallel opportunity to thoroughly examine patterns of flooding.

87 The study area has a total area size of approximately $120,197 \text{ km}^2$. The topography of the study
88 area is divided into regions: the coast, north-central plateaus, and the Niger-Benue rivers
89 (Ighileet. *al.*, 2022). According to the Köppen climate classification system, the study area
90 primarily falls under the Af(tropical rainfall) climate type characterized by high temperature
91 across the year, the relative distribution of abundant rainfall, and lush vegetation. The maximum
92 temperature in the south ranges from 30° C to 32° C , while in the north, the temperature ranges
93 from 33° C to 35° C . The derived savannah, southern Guinea savannah, and humid forest are
94 among the agroecological zones found in the research region. These zones are arranged from the
95 north to the south. The geological features of the study area are primarily the basement complex,
96 which occupies the northern part of the basin and is composed of rocks like schists, granites, and
97 gneisses, and the sedimentary basins, which cover the southern portion of the basin and are
98 composed of rocks like sandstones, shales, and limestones.



100 Figure 1: Location map of the study area

101

102

103

104

105 **3.0 MATERIALS AND METHODS**

106 **3.1 Datasets**

107 The study utilized datasets to map the flood-prone area within the sub-lower Niger River basin of
108 Nigeria. The datasets are highlighted alongside their sources in Table 1. These datasets, their
109 resolutions, and their sources are summarized in Table 1.

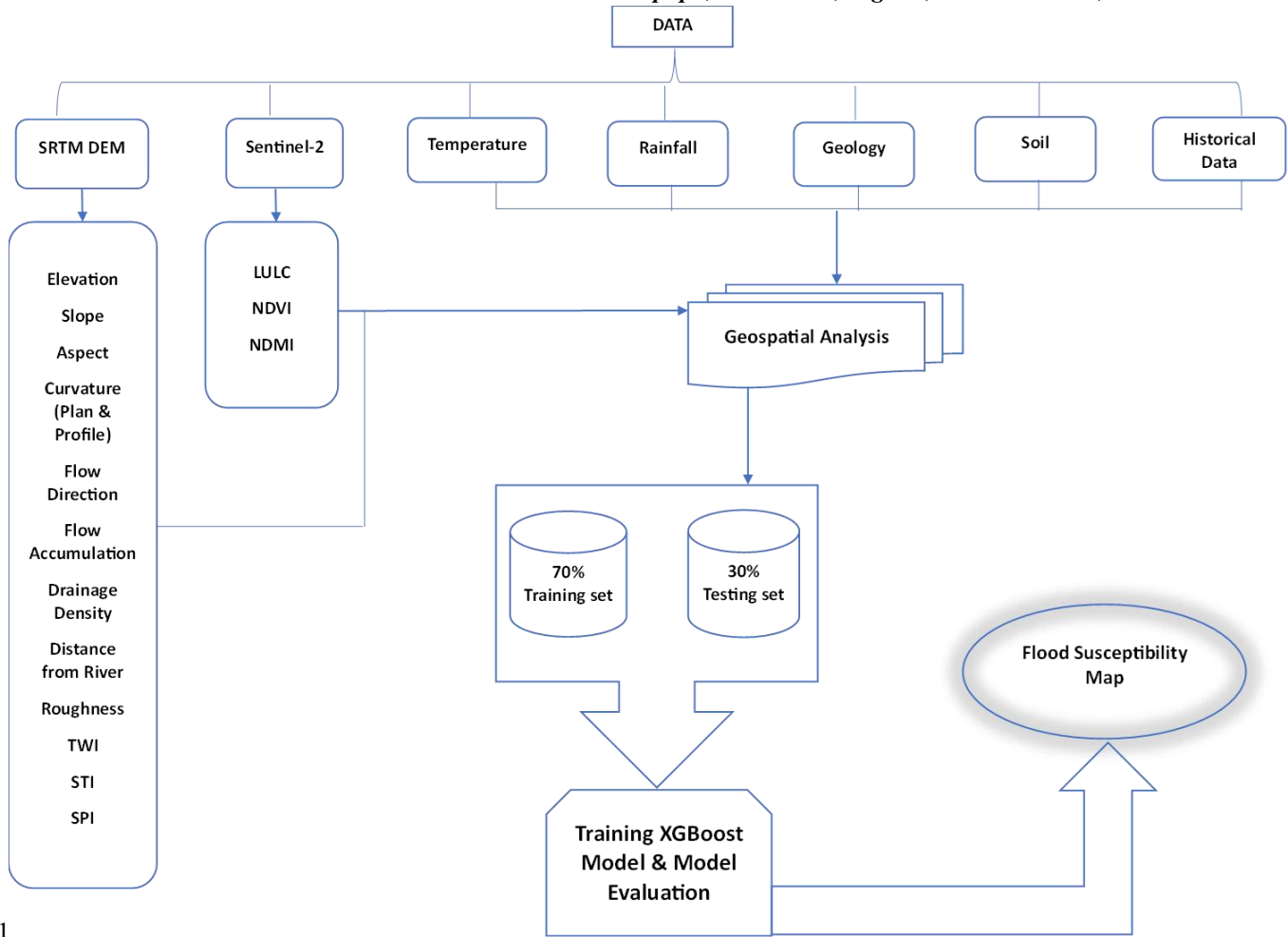
110 **Table 1: Dataset used and their source**

S/N	DATA	RESOLUTION	SOURCE
1.	SRTM DEM Data	30m	USGS Earth Explorer Website
2.	Sentinel-2Satellite Imagery Data	15m	Google Earth Engine
3.	Climate Data	30secs	WorldClim Website
4.	Soil Data	-	FAO Website
5.	Geology Data	-	Nigeria Geological Survey Website

111

112 **3.2 Methods**

113 The methodology adopted to generate the flood susceptibility map of this study is described in
114 the methodology flowchart (Figure 2). The process involved selection of the flood influencing
115 factors to be considered for the flood susceptibility mapping of the study area, acquisitionofdata
116 for theextraction of flood factors and historical data for the flood inventory map, preparationof
117 the flood influencing factors through geospatial analysis, selection suitable factors through
118 multicollinearity investigation, splitting of the dataset for modeling to training sets and testing set,
119 training the XGBoost machine learning model and evaluating the model, and finally, production
120 ofthe flood susceptibility map.



121
122 **Figure 2:** Methodology flowchart of the study

123
124
125
126
127
128
129
130
131
132
133
134
135
136
137
138

3.2.1 Flood Inventory Map

A flood inventory map is crucial in the comprehensive mapping and evaluation of flood hazards in an area (Ghosh *et. al.*, 2023). The flood inventory map of the study area was created utilizing historical flood occurrence data. The historical flood data were collated from various sources, including, the review of literature, satellite imagery, maps and photos of previous floods, and field surveys. A total of 1164 flooded and non-flooded points were collected within the study area, out of which 70% were considered as a training dataset to train the XGBoost machine learning model while the remaining 30% were considered as a testing dataset to validate the model.

3.2.2 Flood Influencing Factors

The flood-influencing factors considered for the prediction of flood susceptible zones in this research were selected based on existing literature by researchers and experts on flood mapping and modeling. The selected flood-influencing factors in this study are categorized into

139 topographic, hydrologic, climatic, and environmental factors. The acquired remotely sensed and
140 geospatial data were prepared for further image processing and analysis was used in producing
141 each factor map. The digital elevation model (DEM) data was used to generate the topographic
142 and hydrologic factors map such as slope, aspect, curvature (plan and profile), topographic
143 wetness index (TWI), sediment transport index (STI), stream power index (SPI), distance from
144 the river, and drainage density.

145 Elevation is regarded in many studies as one of the most crucial variables in flood mapping or
146 modeling since a decrease in elevation increases the probability of flooding in a given location.
147 The slope is another significant factor that influences how surface water flows (Edamoet. *al.*,
148 2022). The degree of slope has an impact on the pace of water infiltration and surface runoff. A
149 region's chance of flooding reduces as its slope decreases. The index of aspects provides a more
150 precise assessment of flood risk mapping (Edamoet. *al.*, 2022). It is well-recognized that low-
151 lying, downslope areas may be more susceptible to floods. Curvature, sometimes referred to as
152 its "slope of slope," (Longley et. al., 2011) was considered for this study. Selecting its two types
153 (plan and profile curvatures), they influence the likelihood of floods by highlighting the
154 divergent and convergent runoff zones. Areas in the study area that are concave and flat have a
155 higher chance of flooding (Ighileet. *al.*, 2022). Using ArcGIS's spatial analyst tools, the slope
156 aspect and both curvature maps were created from the DEM data. Roughness is identified to
157 indicate disparity of elevation between adjoining pixels (Mahdizadeh and Perez, 2022). The map
158 is generated from the DEM data following the equation:

$$Roughness = \frac{(FS_{mean} - FS_{min})}{(FS_{max} - FS_{min})}$$

159 Where, FS_{mean}, FS_{min}, and FS_{max} denote the mean, minimum, and maximum focal statistical
160 layer, respectively.

161 The ability to distinguish between directions of flow is among the essential features of surface
162 hydrology. (Edamoet. *al.*, 2022). The flow direction raster was generated from the fill DEM layer
163 and it was further used to create the flow accumulation map. High flow accumulation indicates
164 areas with a significant volume of water draining through them making the area more susceptible
165 to flooding. The impact of drainage density on the amount of runoff that develops and exits the
166 floodplain area makes it a crucial element in flood susceptibility mapping (Avand *et. al.*,
167 2021). Since places that are susceptible to flooding are often located in close proximity to rivers,
168 mapping flood susceptibility also heavily depends on the distance from the river feature. An
169 individual or feature's likelihood of being impacted by flooding decreases with distance from the
170 river (Liu *et al.*, 2021; Edamoet. *al.*, 2022). The drainage density and distance from the river
171 layers were generated from the stream layer using the density tool and distance tool respectively
172 in ArcGIS. TWI provides a concrete component in research on the incidence of floods since it
173 indicates the amount of water present in a region (Ighileet. *al.*, 2022). An increase in the value of
174 TWI in a given location denotes a significant probability of flooding. The STI which describes
175 the particles in water moving due to water flow was also selected being one of the most
176 important parameters used in flood modeling (Ighileet. *al.*, 2022). Similarly, SPI has a major

177 impact on the hydrologic system (Edamoet. *al.*, 2022). The SPI calculates the erosive power of
178 flowing water (Ighileet. *al.*, 2022). The TWI, STI, and SPI were generated from DEM data using
179 the Raster Calculator tool in ArcGIS according to the following equations respectively:

$$TWI = \ln \frac{\alpha}{\tan\beta}$$

180 Where, α is the upstream discharge at a certain point, and $\tan\beta$ represents the slope in radians.

$$STI = \left(\frac{As}{22.13} \right)^{0.6} \left(\frac{\sin\beta}{0.0896} \right)^{1.3}$$

181 Where, As is the area of the catchment/flow accumulation and β is the slope.

$$SPI = \alpha * \tan\beta$$

182 Where, α is the upstream release at a certain point, and $\tan\beta$ represents the slope in radians.

183 Furthermore, the anthropogenic and environmental factors map including land use/land cover
184 (LULC), normalized difference vegetation (NDVI), and normalized difference moisture index
185 (NDMI) maps were generated from the Sentinel-2 satellite imagery. In addition to being a
186 significant contributing factor to flooding, the LULC was chosen because it clarifies the
187 connection between floods and human activities in the natural environment. The supervised
188 classification method was adopted using Google Earth Engine to classify the Sentinel-2 satellite
189 imagery to generate the LULC map of the study area. The NDVI and NDMI are both vegetation
190 indices used to determine respectively the health and moisture contents of the vegetation in the
191 study area. Using Google Earth Engine, each index map was generated following the equations
192 respectively:

$$NDVI = \frac{NIR - R}{NIR + R}$$

193 Where NIR is the Near Infrared band of Sentinel-2, and R is the Red band of Sentinel-2.

$$NDMI = \frac{NIR - SWIR}{NIR + SWIR}$$

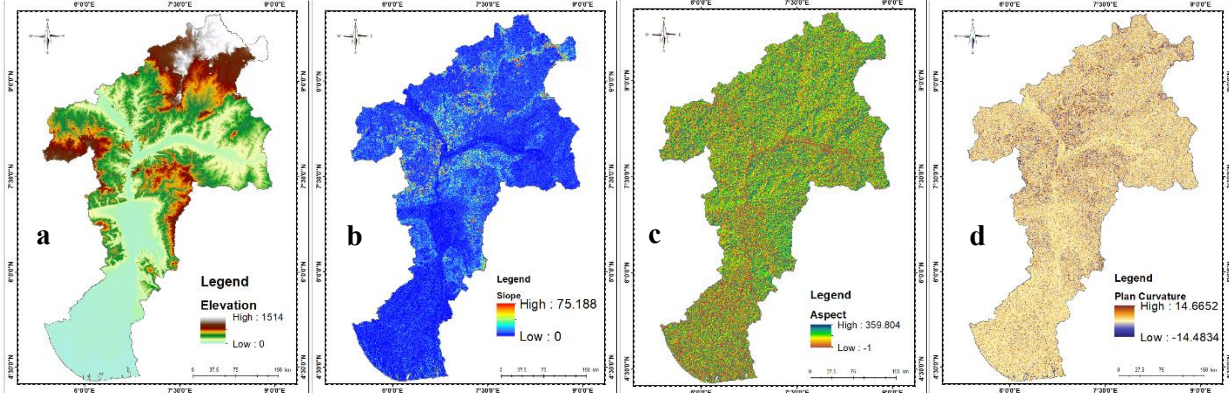
194 Where, NIR is the Near Infrared band of Sentinel-2, and SWIR is the Short-Wave Infrared band
195 of Sentinel-2.

196 Additionally, the soil and geology of the study area were selected for the flood susceptibility
197 mapping. The type of soil of an area affects the drainage process of the area based on the soil
198 characteristics. Soil types with low water permeability porosity or fine texture are known to be
199 highly prone to floods. Similarly, the permeability of rock determines the rate of infiltration of
200 water into the sub-zones.

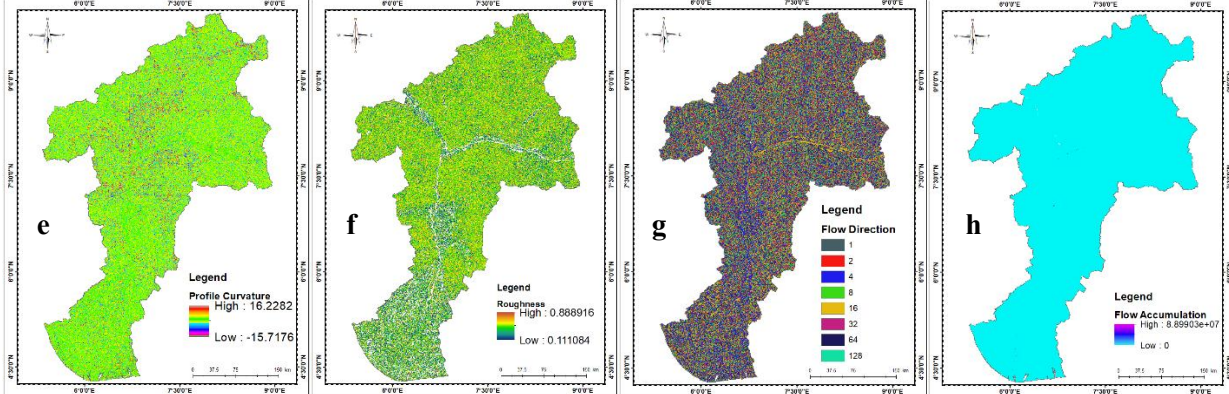
201

*Book of Proceedings, 14th Nigeria Association of Hydrological Sciences Conference
(Okitipupa 2024) held at Olusegun Agagu University of Science and Technology,
Okitipupa, Ondo State, Nigeria, November 5 - 8, 2024*

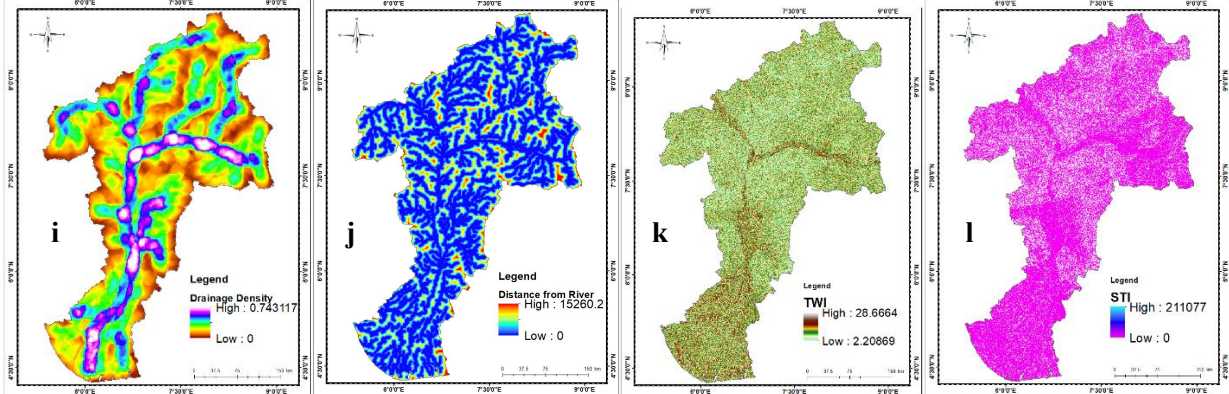
202



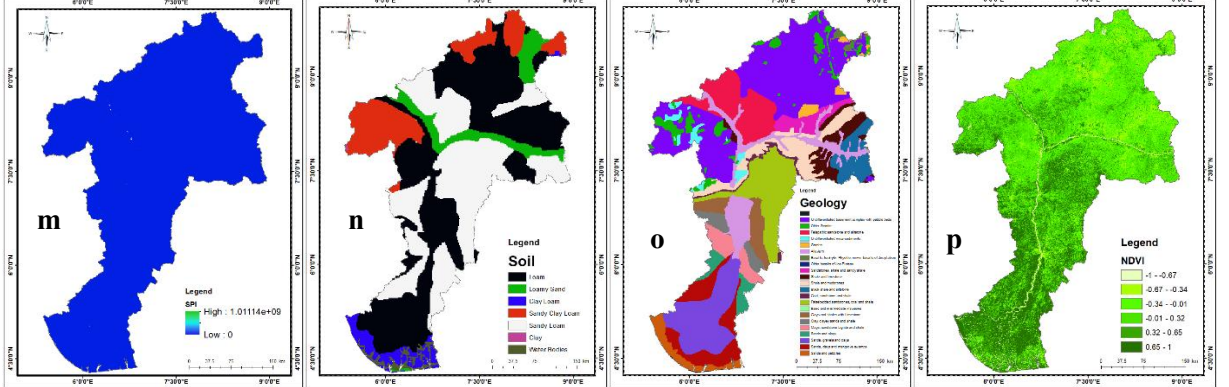
203

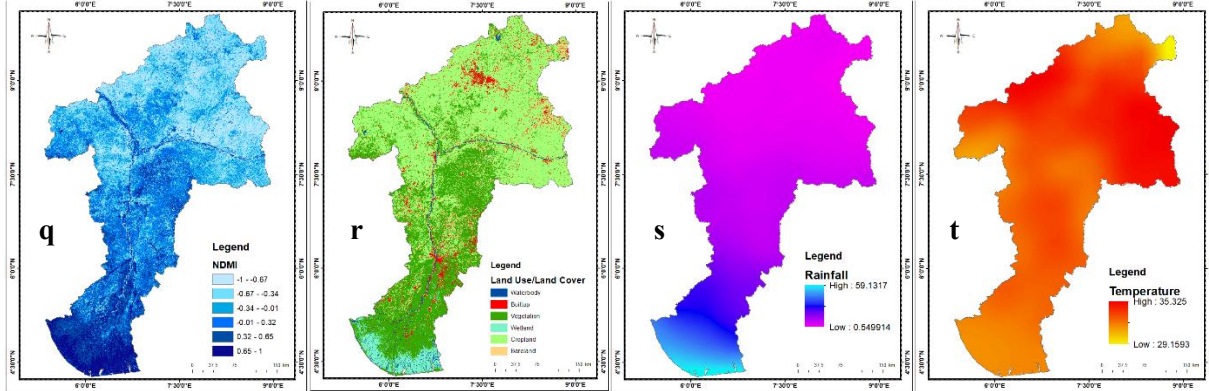


204



205





206
 207 Figure 3: Flood influencing factors (a) Elevation, (b) Slope, (c) Aspect, (d) Plan Curvature, (e)
 208 Profile Curvature, (f) Roughness, (g) Flow Direction, (h) Flow Accumulation, (i) Drainage
 209 Density, (j) Distance from Rivers, (k) Topographic Wetness Index (TWI), (l) Sediment Transport
 210 Index (STI), (m) Stream Power Index (SPI), (n) Soil Types, (o) Geology, (p) Normalized
 211 Difference Vegetation Index (NDVI), (q) Normalized Difference Moisture Index (NDMI), (r)
 212 Land Use/Land Cover (LULC), (s) Annual Rainfall, and (t) Annual Temperature.

213

214 3.2.3 Extreme Gradient Boosting (XGBoost) Machine Learning Model

215 The ensemble machine-learning model, Extreme Gradient Boosting (XGBoost) was put out by
 216 Chen and Guestrin (2016). Through the use of gradient boosting, it applies machine learning
 217 methods to solve problems in parallel via tree-boosting. To prevent overfitting and enhance the
 218 model's capacity for generalization, regularization approaches were employed. The computational
 219 efficiency of the XGBoost algorithm is high. XGBoost can handle missing values, therefore
 220 missing values does not require any particular processing when applying the model (Ren *et. al.*,
 221 2024). In this study, the XGBoost model was implemented in the prediction of the flood hazard
 222 zones of the study area. The 20 flood-influencing factors were considered the independent
 223 variables while the computed inventory data comprising the flooded and non-flooded dataset are
 224 considered the target variable.

225

226 3.2.4 Multicollinearity Investigation

227 Examining the link between variables is essential when making predictions in order to determine
 228 the level of correlation between the variables and ensure high prediction accuracy. When there is
 229 a high correlation between two or more independent variables, multicollinearity occurs which in
 230 turn causes errors in modeling and reduces the accuracy of the result, hence there is a need to
 231 remove one out of the two or two out of the three multicollinear variables leaving one out for
 232 better accuracy. The multicollinearity investigation in this study was conducted using Pearson's
 233 correlation coefficients technique. By pairing all the independent variables, Pearson's correlation
 234 coefficient revealed how strong the linear relationship is between each of them. The Pearson
 235 correlation coefficient is calculated following this formula (Ighile *et. al.*, 2022):

$$r = \frac{\sum(xi - x)(yi - y)}{\sqrt{(\sum(xi - x)^2)(\sum(yi - y)^2)}}$$

236 Where, r is the correlation coefficient, x_i and y_i are the values of variables x and y , and \bar{x} and \bar{y} are
237 the mean values of each variable.

238 The values of the Pearson's correlation coefficient varied from -1 to 1. A perfect positive
239 correlation is represented by a value of 1, a perfect negative correlation by a value of -1, and no
240 correlation is represented by a value of 0. A table referred to as a correlation matrix, which
241 displays the values of the linear associations between each of the independent variables, was
242 used to convey the results of Pearson's correlation coefficient study. From the Pearson correlation
243 coefficient matrix (Table 2), none of the factors shows to be multicollinear. They have no high
244 multicollinearity and strong correlations, making them all necessary for the modeling.

245 **Table 2:** Correlation matrix of the flood influencing factors and the target variable with each
246 causative factor IGR value

247 Factors: 1-Elevation; 2-Aspect; 3-Flow Direction; 4-Flow Accumulation; 5-Drainage Density; 6-
248 Distance from the River; 7-Plan Curvature; 8-Profile Curvature; 9-Roughness; 10-Slope; 11-SPI;
249 12-STI; 13-TWI; 14-Soil; 15-Geology; 16-Precipitation; 17-Temperature; 18-NDMI; 19-NDVI;
250 20-LULC

<i>Factor</i>	<i>Target</i>	1	2	3	4	5	6	7	8	9	10	11	12	13	14
<i>1</i>	0.405	1													
<i>2</i>	0.187	0.242	1												
<i>3</i>	0.038	0.085	0.091	1											
<i>4</i>	0.010	0.103	0.078	0.065	1										
<i>5</i>	0.509	0.496	0.162	0.072	0.054	1									
<i>6</i>	0.250	0.332	0.125	0.058	0.095	0.412	1								
<i>7</i>	-0.006	0.033	0.049	-0.004	0.055	0.030	-0.026	1							
<i>8</i>	0.048	0.044	0.163	0.060	0.088	0.033	0.077	-0.363	1						
<i>9</i>	-0.321	-0.329	-0.349	0.017	-0.038	-0.219	-0.143	-0.087	0.144	1					
<i>10</i>	0.261	0.373	0.249	0.055	0.115	0.252	0.190	0.034	0.152	-0.319	1				
<i>11</i>	0.029	0.196	0.115	0.131	0.335	0.094	0.173	0.100	0.152	0.011	0.271	1			
<i>12</i>	0.211	0.234	0.184	0.009	0.050	0.169	0.103	-0.031	0.089	-0.257	0.473	0.096	1		
<i>13</i>	0.274	0.294	0.333	0.026	0.117	0.201	0.138	0.280	0.005	-0.614	0.519	0.096	0.397	1	
<i>14</i>	-0.060	-0.064	-0.008	0.016	0.024	-0.087	-0.022	0.031	0.020	0.014	0.000	0.074	-0.022	0.011	1
<i>15</i>	0.301	0.248	0.113	0.032	0.065	0.276	0.154	0.077	0.010	-0.139	0.158	0.125	0.144	0.147	-0.060
<i>16</i>	0.056	0.375	0.073	0.002	-	-	0.003	0.017	0.011	-	0.144	-	0.112	0.154	0.417

					0.020	0.020				0.196		0.013			
17	-0.040	-	-	-	-	-	-	0.036	0.021	-	-	-	-	0.052	0.384
		0.102	0.001	0.048	0.028	0.126	0.053			0.052	0.019	0.010	0.010		
18	0.062	0.226	0.045	-	0.031	-	0.037	-	-	-	0.069	0.008	0.065	0.102	0.216
				0.026		0.010		0.011	0.007	0.158					
19	0.026	-	0.035	0.030	0.051	0.069	0.022	0.027	0.030	0.026	0.020	-	-	-	0.083
		0.089										0.013	0.004	0.001	
20	0.020	0.127	0.033	-	0.054	-	-	0.044	0.016	-	0.005	0.017	0.058	0.100	0.126
				0.049		0.052	0.002			0.138					

251

252

253 **3.2.5 Model Training and Evaluation**

254 Training of a machine learning model can be described as the act of feeding the machine learning
 255 algorithm with labeled data to make it discover the underlying patterns and correlations of the
 256 dataset. To help the model understand the relationships and patterns in the dataset, the data must
 257 be exposed to the model. For the implementation of the XGBoost model, the computed dataset
 258 was split into a training dataset and a testing dataset in a 70:30. The training dataset was used to
 259 train the model, and the testing dataset was used to test the model. Analyzing the training dataset
 260 reveals a dataset's fitness while analyzing the testing dataset reveals the model's prediction ability
 261 (Bhattarai *et. al.*, 2024). Accuracy, f1-score, recall, precision, and ROC-AUC were used to
 262 evaluate and validate the model performance.

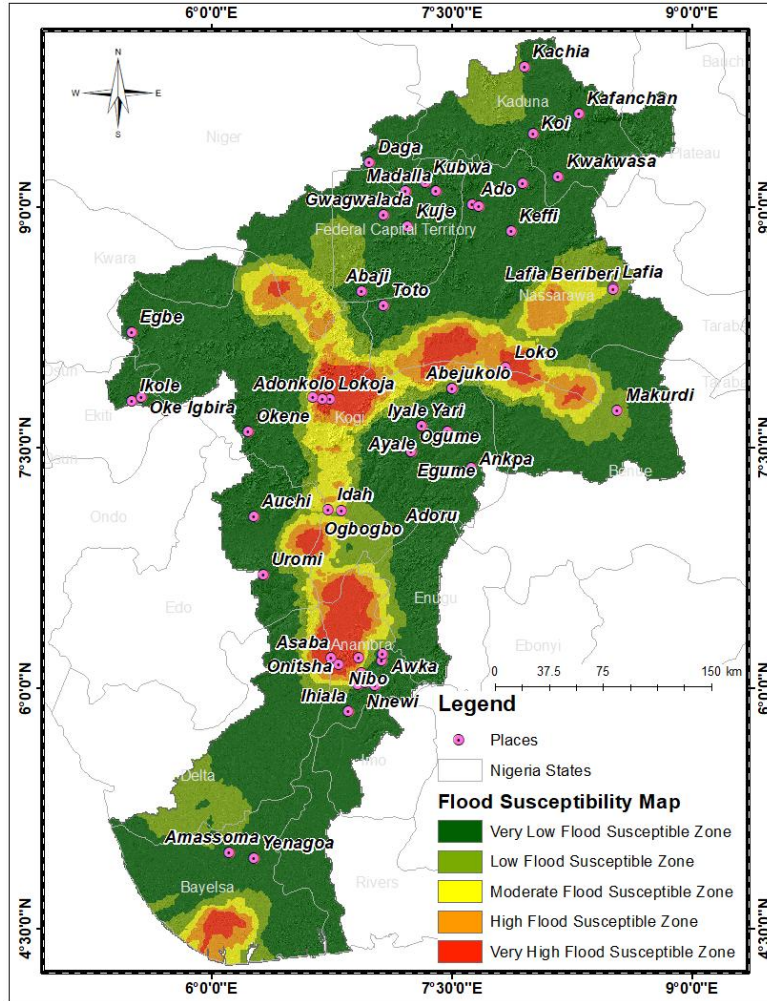
263

264 **4.0 RESULTS**

265 **4.1 Flood Susceptibility Map**

266 The mapping of flood susceptibility involves predicting the likelihood of flooding in different
 267 areas, while floodplain maps show where water will go based on past events. The generated flood
 268 susceptibility map of the study area is shown in Figure 4. Based on the natural breaks'
 269 classification method in ArcGIS, the flood susceptibility map was classified into five
 270 susceptibility zones: very low, low, moderate, high, and very high. Major cities and towns within
 271 the study area and States of the country were overlaid on the flood susceptibility layer.

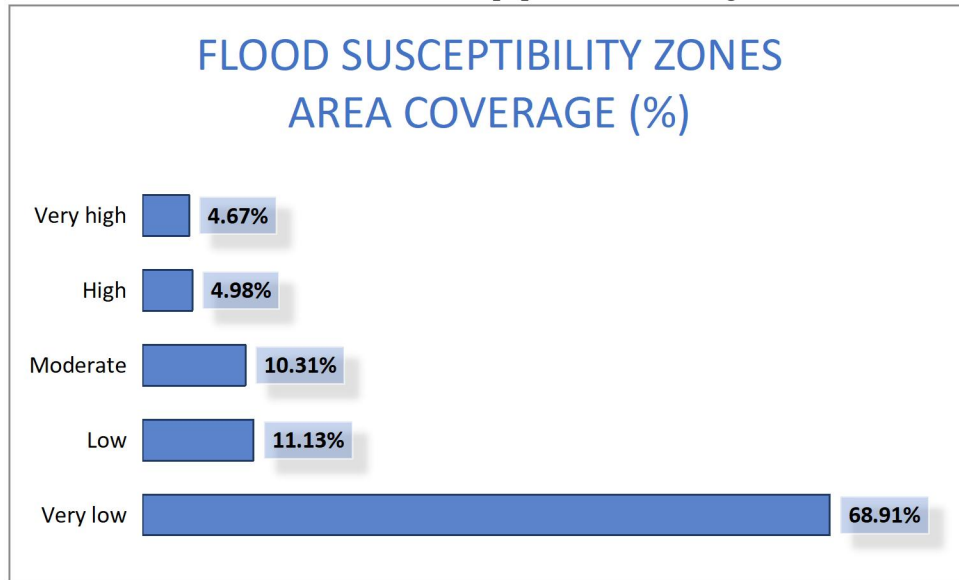
272 It can be inferred from the resultant map that there is a non-uniform distribution of flood
 273 susceptibility across the study area. The study identified the central region states such as Kogi
 274 State (being the confluence area of the Niger and Benue Rivers), the Nasarawa State, the Delta-
 275 Anambra States region, and some southern region; coastal states of the study area to majorly
 276 exhibit higher susceptibility to flooding. In quantifying the area coverage of each susceptibility
 277 classes, 4.67% of the area is under the very high susceptible zone, followed by 4.98% under the
 278 high susceptible zone, 10.31% under the moderate susceptible zone, 11.13% under the low
 279 susceptible zone, and the very low susceptible zone taking the largest area of 68.91% of the
 280 study area (Table 3).



281
282 Figure 4: Flood Susceptibility Map

283
284 **Table 3: Percent and Area extent of each susceptibility zone**

<i>Susceptibility Zone</i>	<i>Area Extent (km²)</i>	<i>Percent (%)</i>
<i>Very low</i>	82704.00	68.91
<i>Low</i>	13354.35	11.13
<i>Moderate</i>	12374.91	10.31
<i>High</i>	5981.12	4.98
<i>Very high</i>	5607.63	4.67



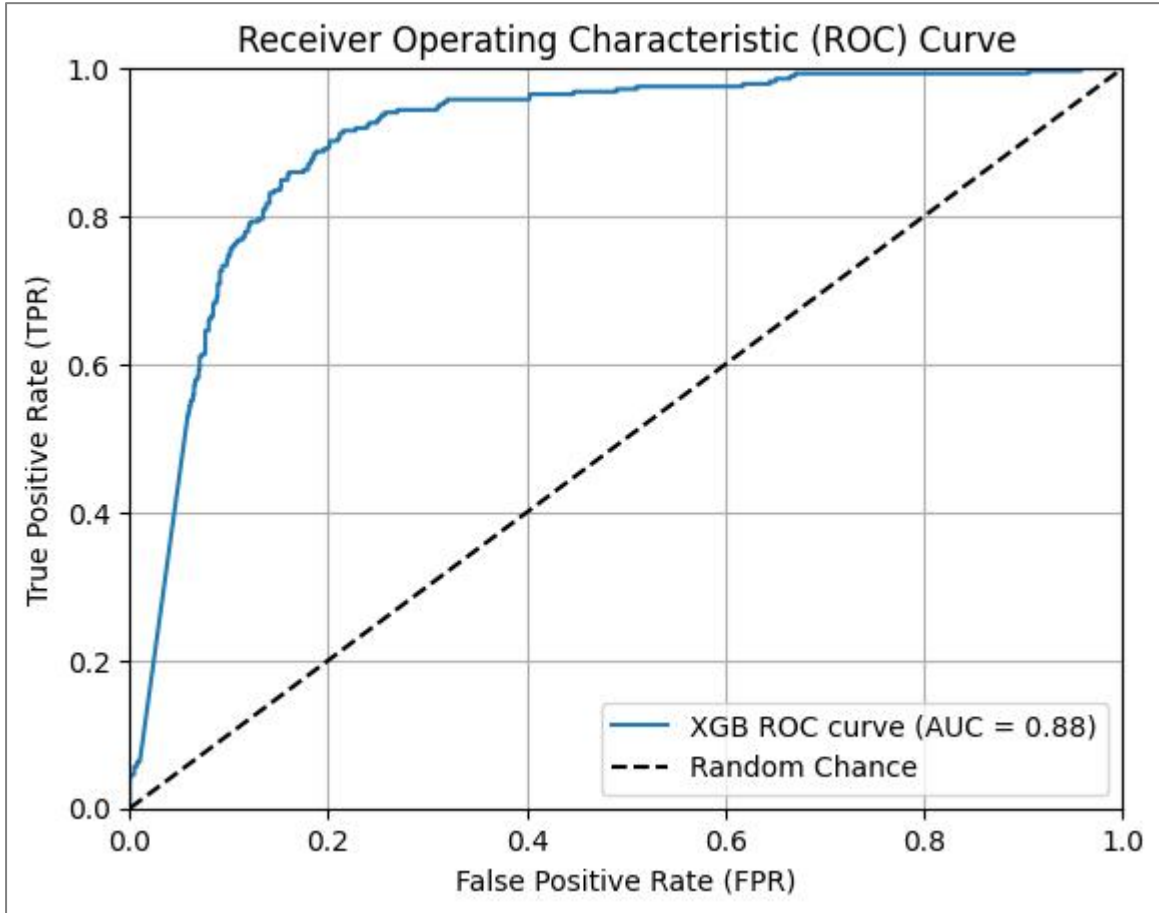
286
287 Figure 5: Chart showing the percentage of flood susceptible zones in the study area
288

289 **4.2 Model Performance Evaluation and Validation**

290 The result from the evaluation and validation of the model used for the flood susceptibility
291 mapping shows a high performance of the model. The indicators used for the evaluation of the
292 model’s performance are precision, recall, f1-score, accuracy, and receiver operating
293 characteristics-area under the curve (ROC-AUC). The model presented an overall accuracy of
294 90.5% while the precision, recall, and f1-score presented similar values of 0.94 and 0.81 for the
295 non-flooded (0) and flooded points datasets respectively (Table 4). The receiver operating
296 characteristics area under the curve (ROC-AUC) score is shown to be 0.88 (Figure 6).

297 **Table 4: Performance parameters of the machine learning model**

<i>ML Model</i>	Flood Status	Precision	Recall	F1-Score	Accuracy
<i>XGBoost</i>	0	0.94	0.94	0.94	90.5%
	1	0.81	0.81	0.81	



300

301 Figure 6: ROC-AUC plot of the machine learning model used for flood susceptibility mapping

302

303 5.0 DISCUSSION

304 The provision of the necessary spatial framework by GIS for data management, data analysis,
305 and data visualization, and the strive by a machine learning algorithm to extract valuable insights
306 from the geospatial and hydrological information aided a great deal in predicting and mapping
307 flood-prone areas in the study area. Integration of GIS and machine learning techniques proved
308 to be a powerful and valuable approach to enhancing flood hazard mapping. Given that the Niger
309 River in Nigeria, Benue River being its main tributary, experiences flooding annually, hence
310 mapping the degree of flood hazard in the river basin is important. Different studies have utilized
311 machine learning techniques with GIS techniques to predict and map hazards such as flood
312 (Ighileet. *al.*, 2022; Bhattarai *et. al.*, 2024), drought (Alawsiet. *al.*, 2022), and groundwater
313 (Nourani and Mousavi, 2016).

314 In this study, the effectiveness of combining machine learning and GIS to generate enhanced
315 results in flood hazard prediction was demonstrated. The extreme gradient boosting (XGBoost)
316 model was applied to predict the flood hazard zones in the study area. Twenty factors influencing
317 flood in the Niger River basin were used to produce the flood hazard map of the study area.
318 Rainfall, flow accumulation, elevation, distance from the river, slope, and land use/land cover
319 factors were demonstrated to be some of the most significant factors impacting floods in the area.

320 Rainfall as a dynamic factor has a significant impact on floods in the study area. The part of the
321 Niger River in Nigeria which is downstream of the whole river suffers from flooding majorly
322 during the rainfall season mostly when there is heavy rainfall at the upstream causing overflow
323 downstream of the river. The accumulation of water flow from the upstream proves its effect
324 mostly at the confluence area (i.e. Kogi State), the Delta-Anambra State, and the coastal area of
325 the study area. Elevation and slope are also critical factors influencing floods in the study area.
326 The speed and volume of runoff in the study area are relatively due to the elevation and steepness
327 of the slope of the study area. The proximity to the low-lying river determines the level of risk to
328 the flood hazard. In areas with dense land cover such as forests, the speed and amount of
329 runoff and the resulting damage decrease (Avand *et. al.*, 2021). The increase in urbanization over
330 time causing deforestation exposed the study area to flooding. The activities of humans such as
331 settlements, farming, etc. increase the high susceptibility to flood in the areas. Due to the
332 extensive activities of humans in Nigeria, flood probability may worsen over time (Ighileet *al.*,
333 2022).

334 The XGBoost machine learning model evaluation proves the high performance of the model in
335 this study, hence it's useful in mapping flood-prone areas in other studies. Incorporating
336 additional data sources such as high-resolution imagery, and real-time hydrological data, could
337 improve the model performance and provide more detailed flood predictions.

338

339 **6.0 CONCLUSION**

340 Leveraging the strengths of GIS and machine learning techniques, this study predicted and
341 produced the flood susceptibility map of the study area. Twenty flood influencing factors which
342 are elevation, slope, aspect, flow direction, flow accumulation, drainage density, distance from
343 river, plan curvature, profile curvature, roughness, topographic wetness index (TWI), stream
344 power index (SPI), sediment transport index (STI), normalized difference vegetation index
345 (NDVI), normalized difference moisture index (NDMI), land use/land cover (LULC), soil,
346 geology, temperature, and rainfall, were selected to successfully develop the flood susceptibility
347 map.

348 A flood inventory map was initially created using historical flood occurrences data in Nigeria.
349 The generated data were further divided into 70% training dataset and 30% testing dataset.
350 Indicators such as precision, recall, f1-score, accuracy, and ROC-AUC were used to evaluate the
351 performance of the XGBoost machine learning model. The model having a high-performance
352 accuracy of 90.5% and a ROC-AUC score of 0.88. The flood susceptibility map developed in
353 this study help highlight areas that are prone to flooding in the study area ranking the
354 susceptibility between low to high levels. The successful integration of GIS with machine
355 learning validates the potential to improve flood hazard prediction and mitigation efforts in the
356 Niger River basin and other similar flooding environments in Nigeria. The findings from this
357 study, proves the effectiveness of the integration as a relevant approach for academic and
358 policymakers in comprehending flood occurrences. One of the limitations of this study is the
359 lack of access to some areas for field survey. However, this study suggests that further similar

360 research should focus on refining machine learning model by incorporating additional variable,
361 and comparing different models for the flood hazard mapping.

362

363 REFERENCES

- 364 Ajin, R.S., R.R. Krishnamurthy, M. Jayaprakash and P.G. Vinod. (2013). Flood hazard
365 assessment of Vamanapuram River Basin, Kerala, India: An approach using Remote
366 Sensing & GIS techniques. *Advances in Applied Science Research*. 4. 263-274.
- 367 Alawsi, M.A.; Zubaidi, S.L.; Al-Bdairi, N.S.S.; Al-Ansari, N.; Hashim, K. Drought Forecasting:
368 A Review and Assessment of the Hybrid Techniques and Data Pre-Processing. *Hydrology*
369 2022, 9, 115. <https://doi.org/10.3390/hydrology9070115>
- 370 Avand, M., Moradi, H. R., &Lasboyee, M. R. (2021). Spatial Prediction of Future Flood Risk:
371 An Approach to the Effects of Climate Change. *Geosciences*, 11(1), 25.
372 <https://doi.org/10.3390/geosciences11010025>
- 373 Bhattarai, Y., Duwal, S., Sharma, S., &Talchabhadel, R. (2024). Leveraging machine learning
374 and open-source spatial datasets to enhance flood susceptibility mapping in transboundary
375 river basin. *International Journal of Digital Earth*,
376 17(1).<https://doi.org/10.1080/17538947.2024.2313857>
- 377 Cabrera, N., & Lee, N. (2019). Flood-Prone Area Assessment Using GIS-Based Multi-Criteria
378 Analysis: A Case Study in Davao Oriental, Philippines. *Water*, 11(11), 2203.
379 <https://doi.org/10.3390/w11112203>
- 380 Edamo, M. L., Ukumo, T. Y., Lohani, T. K., Ayana, M. T., Ayele, M. A., Mada, Z. M., & Abdi, D.
381 M. (2022). A comparative assessment of multi-criteria decision-making analysis and
382 machine learning methods for flood susceptibility mapping and socio-economic impacts on
383 flood risk in Abela-Abaya floodplain of Ethiopia. *Environmental Challenges*, 9, 100629.
384 <https://doi.org/10.1016/j.envc.2022.100629>
- 385 Etuonovbe A. K. (2011). The devastating effect of flooding in Nigeria. In FIG Working Week.
386 2011, May. Accessed 10 March 2015; Available at:
387 http://www.fig.net/pub/fig2011/papers/ts06j/ts06j_etuonovbe_5002.pdf.
- 388 Ghosh, A., Chatterjee, U., Pal, S. C., Islam, A. R. M. T., Alam, E., & Islam, M. K. (2023). Flood
389 hazard mapping using GIS-based statistical model in vulnerable riparian regions of sub-
390 tropical environment. *Geocarto International*, 38(1).
391 <https://doi.org/10.1080/10106049.2023.2285355>
- 392 Ibitoye, M. O., Komolafe, A. A., Adegboyega, A. a. S., Adebola, A. O., & Oladeji, O. D. (2019).
393 Analysis of vulnerable urban properties within river Ala floodplain in Akure, Southwestern
394 Nigeria. *Spatial Information Research*, 28(4), 431–445. [https://doi.org/10.1007/s41324-](https://doi.org/10.1007/s41324-019-00298-6)
395 [019-00298-6](https://doi.org/10.1007/s41324-019-00298-6)
- 396 Ighile, E.H.; Shirakawa, H.; Tanikawa, H. Application of GIS and Machine Learning to Predict
397 Flood Areas in Nigeria. *Sustainability* 2022, 14, 5039. <https://doi.org/10.3390/su14095039>

- 398 Komolafe, A. A., Adegboye, S. a. A., & Akinluyi, F. O. (2015). A Review of Flood Risk
399 Analysis in Nigeria. *American Journal of Environmental Sciences*, 11(3), 157–166.
400 <https://doi.org/10.3844/ajessp.2015.157.166>
- 401 Maharjan, M., Timilsina, S., Ayer, S., Singh, B., Manandhar, B., & Sedhain, A. (2024). Flood
402 susceptibility assessment using machine learning approach in the Mohana-Khutiya River of
403 Nepal. *Natural Hazards Research*. <https://doi.org/10.1016/j.nhres.2024.01.001>
- 404 Mahdizadeh Gharakhanlou, N.; Perez, L. Spatial Prediction of Current and Future Flood
405 Susceptibility: Examining the Implications of Changing Climates on Flood Susceptibility
406 Using Machine Learning Models. *Entropy* 2022, 24,
407 1630. <https://doi.org/10.3390/e24111630>
- 408 Mojaddadi, H., Pradhan, B., Nampak, H., Ahmad, N., & Ghazali, A. H. B. (2017). Ensemble
409 machine-learning-based geospatial approach for flood risk assessment using multi-sensor
410 remote-sensing data and GIS. *Geomatics Natural Hazards and Risk*, 8(2), 1080–1102.
411 <https://doi.org/10.1080/19475705.2017.1294113>
- 412 Morjani, Z. E. a. E., Ennasr, M. S., Elmouden, A., Idbraim, S., Bouaakaz, B., & Saad, A. (2016).
413 Flood Hazard Mapping and Modeling Using GIS Applied to the Souss River Watershed. In
414 *The handbook of environmental chemistry* (pp. 57–93).
415 https://doi.org/10.1007/698_2016_69
- 416 Nguyen, D., Chou, T., Hoang, T., & Chen, M. (2023). Flood Susceptibility Mapping Using
417 Machine Learning Algorithms: A Case Study in Huong Khe District, Ha Tinh Province,
418 Vietnam. *International Journal of Geoinformatics*, 1–15.
419 <https://doi.org/10.52939/ijg.v19i7.2739>
- 420 Nourani, V.; Mousavi, S. Spatiotemporal groundwater level modeling using hybrid artificial
421 intelligence-meshless method. *J. Hydrol.* 2016, 536, 10–25.
422 <http://doi.org/10.1016/j.jhydrol.2016.02.030>
- 423 Park, S. J., & Lee, D. K. (2020). Prediction of coastal flooding risk under climate change impacts
424 in South Korea using machine learning algorithms. *Environmental Research Letters*, 15(9),
425 094052. <https://doi.org/10.1088/1748-9326/aba5b3>
- 426 Ren, H.; Pang, B.; Bai, P.; Zhao, G.; Liu, S.; Liu, Y.; Li, M. Flood Susceptibility Assessment with
427 Random Sampling Strategy in Ensemble Learning (RF and XGBoost). *Remote Sens.* 2024,
428 16, 320. <https://doi.org/10.3390/rs16020320>
- 429 Tokunbo, A., & Ezigbo, B. (2012). Floods Claims 363 Lives, Displace 2.1 People Says NEMA
430